An Epigenetic Genome-Wide Screen Identifies *SPINT2* as a Novel Tumor Suppressor Gene in Pediatric Medulloblastoma

Paul N. Kongkham,[1] Paul A. Northcott,[2] Young Shin Ra,[1] Yukiko Nakahara,[2] Todd G. Mainprize,[1] Sidney E. Croul,[3] Christian A. Smith,[1] Michael D. Taylor,[2] and James T. Rutka[1]

[1]Program in Cell Biology and [2]Program in Developmental and Stem Cell Biology, Division of Neurosurgery, Arthur and Sonia Labatt Brain Tumor Research Centre, Hospital for Sick Children, and [3]Department of Pathology, University Health Network, University of Toronto, Toronto, Ontario, Canada

Abstract

Medulloblastoma (MB) is a malignant cerebellar tumor that occurs primarily in children. The hepatocyte growth factor (HGF)/MET pathway has an established role in both normal cerebellar development as well as the development and progression of human brain tumors, including MB. To identify novel tumor suppressor genes involved in MB pathogenesis, we performed an epigenome-wide screen in MB cell lines, using 5-aza-2′deoxycytidine to identify genes aberrantly silenced by promoter hypermethylation. Using this technique, we identified an inhibitor of HGF/MET signaling, *serine protease inhibitor kunitz-type 2* (*SPINT2/HAI-2*), as a putative tumor suppressor silenced by promoter methylation in MB. In addition, based on single nucleotide polymorphism array analysis in primary MB samples, we identified hemizygous deletions targeting the *SPINT2* locus in addition to gains on chromosome 7 encompassing the *HGF* and *MET* loci. *SPINT2* gene expression was down-regulated and *MET* expression was up-regulated in 73.2% and 45.5% of tumors, respectively, by quantitative real-time PCR. *SPINT2* promoter methylation was detected in 34.3% of primary MBs examined by methylation-specific PCR. *SPINT2* reexpression in MB cell lines reduced proliferative capacity, anchorage independent growth, cell motility *in vitro*, and increased overall survival times *in vivo* in a xenograft model ($P < 0.0001$). Taken together, these data support the role of *SPINT2* as a putative tumor suppressor gene in MB, and further implicate dysregulation of the HGF/MET signaling pathway in the pathogenesis of MB. [Cancer Res 2008;68(23):9945–53]

Introduction

Central nervous system tumors are the most common form of pediatric solid malignancy, with medulloblastoma (MB) accounting for 25% of cases (1, 2). This cerebellar tumor affects young children, with a peak incidence at the age of 7 years and 5-year survival of ~60% (3). Treatment includes a combination of surgery, radiation, and chemotherapy—therapies with significant neurocognitive, endocrinologic, hematologic, and oncologic side effects (4–7).

Although MB typically arise sporadically, some cases occur in family cancer syndromes such as nevoid basal cell carcinoma syndrome or Turcot syndrome—with mutations in the Hedgehog transmembrane receptor *Patched* (*PTCH*) or the Wnt signaling member *APC*, respectively (8, 9). *PTCH* mutations are found in ~10% of sporadic MB cases (10). Other Hedgehog pathway members (*HSUFU, SMO*, and *PTCH2*) are implicated in fewer cases (11–13). *APC* mutations occur infrequently in sporadic MB, although activating mutations of *β-catenin* are seen in up to 5% of cases (14). *MYC* family amplifications occur in <10% of cases (15). Known genetic abnormalities explain tumorigenesis for only a subset of sporadic MB cases. The identification of novel genes and pathways involved in MB pathogenesis may help to explain the etiology of tumors in the remainder of cases, as well as to provide novel targets for therapy.

The role of the HGF/MET signal transduction pathway in the formation and progression of brain tumors including malignant gliomas is well-established (16). It also plays a critical role in cerebellar development (17). Furthermore, the HGF/MET pathway has recently been implicated in MB pathogenesis (15, 18, 19).

To identify novel genes involved in MB pathogenesis that have escaped detection by conventional genetic analysis, we used a genome-wide epigenetic screen to discover putative tumor suppressor genes (TSG) silenced by promoter-region methylation. This approach involved up-regulating epigenetically silenced genes using 5-aza-2′deoxycytidine (5-aza-dC) treatment, followed by expression microarray analysis (20–22). As aberrant promoter methylation may function alone or in concert with genetic events such as loss of heterozygosity (LOH) to induce TSG silencing, we cross-referenced our microarray data with data from a high resolution Affymetrix SNP-array platform to identify genes targeted by methylation and/or LOH events (23). Using this approach, we identified methylation-mediated gene silencing and hemizygous deletion of *SPINT2* in MB. *SPINT2* normally functions to inhibit the HGF/MET signaling pathway. We hypothesized that up-regulated HGF/MET signaling resulting from loss of normal pathway inhibition due to *SPINT2* silencing contributes to MB pathogenesis. Functional analysis *in vitro* and *in vivo* support the role of *SPINT2* as a putative novel TSG in MB.

Materials and Methods

Cell lines, cell culture, and normal cerebellar samples. The ONS76 cell line was obtained from the Institute for Fermentation. The UW228 and UW426 cell lines were obtained from Dr. J. Silber (University of Washington, Seattle, WA). The D425 and D458 cell lines were obtained from Dr. D. Bigner (Duke University, Durham, NC). The MHH-MED-1 and MED8A cell lines were obtained from Dr. R. Gilbertson (St. Jude Children's Research Hospital, Memphis, TN). The RES262 cell line was obtained from Dr. M.S. Bobola (University of Washington, Seattle, WA). All other cell lines were purchased from the American Type Culture Collection. Daoy, D283, ONS76, UW228, and UW426 cell lines were cultured in DMEM with 10% fetal bovine serum (FBS). The D425 and D458 cell lines were cultured in IMEM with 20% FBS,

Note: Supplementary data for this article are available at Cancer Research Online (http://cancerres.aacrjournals.org/).

Requests for reprints: James T. Rutka, The Division of Neurosurgery, Suite 1503, The Hospital for Sick Children, 555 University Avenue, Toronto, Ontario, Canada M5G 1X8. Phone: 416-813-6425; Fax: 416-813-4975; E-mail: james.rutka@sickkids.ca.

doi:10.1158/0008-5472.CAN-08-2169

5 cc of 1 mol/L HEPES, and 15 CC of 7.5% sodium bicarbonate. MHH-MED-1 was cultured in DMEM with 10% FBS, and MED8A in DMEM with 20% FBS. The RES262 MB cell line was cultured in DMEM/F12 medium supplemented with 2% FBS. RKO (colorectal cancer) and PFSK (supratentorial PNET) cell lines were cultured in DMEM with 10% FBS. The G401 cell line (rhabdoid tumor) was cultured in DMEM/F12 with 10% FBS. Lymphoblasts were cultured in RPMI 1640 with 15% FBS. Medium and reagents for cell culture were purchased from Wisent, Inc. Normal human fetal and adult cerebellar genomic DNA and RNA samples were purchased from Biochain.

5-aza-dC treatment protocol, reverse transcription-PCR/quantitative real-time PCR, and affymetrix HG U133 plus 2.0 expression arrays. Cell lines were plated at 20% to 30% confluence. Twenty-four hours later, medium was replaced with fresh medium containing 5 μmol/L 5-aza-dC (Sigma-Aldrich, Inc.) or an equal volume of vehicle (1× PBS). Medium and drug or vehicle were replaced every 24 h over a 72-h period. RNA was extracted using TRIzol reagent (Invitrogen) and quantitated spectrophotometrically by NanodDrop ND-1000 (NanoDrop). cDNA was prepared using 2 μg of total RNA, random hexamer primers, and the Omniscript RT kit (Qiagen, Inc.). Reverse transcription-PCR (RT-PCR) was performed using Platinum Taq DNA Polymerase (Invitrogen) in an MJ Research PTC-200 thermal cycler (Bio-Rad). Quantitative real-time RT-PCR (qRT-PCR) was performed using Platinum SYBR Green Supermix (Invitrogen), in an MJ Research PTC-200 thermal cycler fitted with a Chromo4 detector (Bio-Rad). Primer sequences for RT-PCR and qRT-PCR were as follows: *SPINT2*-F, 5′-aacagcaataattacctgacc-3′; *SPINT2*-R, 5′-aaggatgcacggcaaggc-3′; *MET*-F, 5′-cactgctttaataggacacttctg-3′; *MET*-R, 5′-ggtggatatagatgttaagaggac-3′; *HGF*-F, 5′-ctatgcagagggacaaagga-3′; and *HGF*-R 5′-ccacttgacatgctattgaagg-3′. Expression levels for the *ACTB* gene were used for normalization of relative gene expression levels.

Cell lines were subjected to expression profiling after 5-aza-dC or vehicle treatment using the Affymetrix HG U133 plus 2.0 platform (Affymetrix). As described above, total RNA was extracted using TRIzol, and RNA was quality checked by Bioanalyzer. Array hybridization was performed by our local genomics facility (The Center for Applied Genomics, TCAG, The Hospital for Sick Children, Toronto, Canada). Data analysis was done using the Affymetrix GeneChip Operating Software (GCOS) software for normalization and pairwise comparison between individual 5-aza-dC–treated and untreated cell lines, and filtered to identify genes of interest for further study using the Inforsense KDE program.

DNA isolation from tumor samples and single nucleotide polymorphism GeneChip mapping array analysis. Fresh-frozen MB specimens were stored at −80°C before extraction of nucleic acid. Samples were pulverized under liquid nitrogen. For genomic DNA isolation, ~25 to 50 mg of crushed tissue was subjected to SDS/Proteinase K digestion (Roche) for 3 h at 50°C. Homogenates were extracted thrice with buffer-saturated phenol (Invitrogen) before precipitation of DNA with 2 volumes of anhydrous ethanol and 10% (vol/vol) 10 mol/L ammonium acetate. Precipitated DNA was washed thrice with 70% ethanol and resuspended in reduced EDTA-TE [10 mmol/L Tris, 0.1 mmol/L EDTA (pH 8.0)]. Samples were quantitated by NanoDrop ND-1000, and DNA integrity was assessed by agarose gel electrophoresis before submission for SNP array analysis.

Single nucleotide polymorphism (SNP) array genotyping was performed using the Affymetrix 50 K Hind 240 and 50 K Xba 240, or the 250 K Nsp and 250 K Sty GeneChip Mapping arrays as directed by the manufacturer (Affymetrix). Briefly, 250 ng of DNA was digested with HindIII, XbaI, NspI, or StyI (New England Biolabs), adapter-ligated, and PCR amplified using a single primer with AmpliTaq Gold (Applied Biosystems). Amplified PCR products were pooled, concentrated, and fragmented with DNAase I. Products were then labeled and hybridized overnight to the respective arrays. Arrays were washed using an Affymetrix GeneChip Fluidics Station 450 and scanned using the GeneChip Scanner 3000 7G. CEL files were generated using the Affymetrix GCOS 3.0.

Bisulfite genomic sequencing. The technique of bisulfite genomic sequencing has been previously described (24). Briefly, genomic DNA was subjected to bisulfite conversion using the MethylEasy DNA Bisulfite Modification kit (Human Genetic Signatures). After bisulfite conversion, the *SPINT2* promoter region was amplified using bisulfite-PCR methods. Primer sequences for *SPINT2* bisulfite-PCR were as follows: Fwd 5′-GTTTTG-TTTAGTTAGGTGCGTT-3′, Rev 5′-AAACTCTCCTAACCCTCGCT-3′. PCR products were gel-purified, TA were cloned into pCR2.1 vector (Topo TA Cloning kit; Invitrogen), transformed into TOP10 chemically competent cells, and plated under antibiotic selection. Plasmid DNA from isolated colonies was extracted by miniprep (Qiagen) and sequenced to determine *SPINT2* methylation status. Multiple clones were sequenced, providing a consensus of the promoter-region methylation status. Bisulfite sequencing data were analyzed using BiQ Analyzer software (25).

Methylation-specific PCR. Methylation-specific PCR (MSP) was performed as previously described (26). Published MSP primer pairs designed to specifically amplify either unmethylated or methylated *SPINT2* promoter-region DNA after bisulfite conversion were used (27). Genomic DNA from a panel of 70 primary MB samples was isolated using a standard SDS-proteinase K technique, and subjected to bisulfite conversion. MSP was performed on this panel of tumor samples, in addition to the MB cell line D283 (positive control for *SPINT2*-MSP primers) and three normal human cerebellar samples (positive controls for *SPINT2*-USP primers). Template-negative samples and samples containing genomic DNA not subjected to bisulfite conversion were used as negative controls for both *SPINT2*-MSP and *SPINT2*-USP primer sets.

***SPINT2* expression construct and stable cell line generation.** A plasmid containing full-length human *SPINT2* cDNA was obtained from the Mammalian Gene Collection (*SPINT2*-IRAU5-A9 in pOTB7). After the PCR-mediated addition of a COOH-terminal FLAG tag sequence, this cDNA was subcloned into the pcDNA3.1+ expression vector (Invitrogen), and sequence verified. Empty pcDNA3.1+ and an enhanced green fluorescent protein (EGFP)-pcDNA3.1+ expression construct were used as negative controls. To produce stable transfectants, expression vectors were linearized, transfected into the D283 and ONS76 MB cell lines using FuGene6 (Roche), and kept under G418 antibiotic selection. Transfected cells were subsequently plated into 96-well plates at 1 cell per well, and expanded to obtain stably transfected clones. Two stable D283 clones reexpressing *SPINT2* (D283-*SPINT2*-FLAG-High and D283-*SPINT2*-FLAG-Low) and one ONS76 clone (ONS76-*SPINT2*-FLAG) were selected for further study, with *SPINT2* expression levels verified at both the transcript and protein levels by qRT-PCR and Western blotting (Supplementary Figs. S1 and S2).

Western blotting. Monoclonal anti-FLAG M2 antibody (Sigma-Aldrich F3165) was used for SDS-PAGE. An immunoblot for the transferrin receptor was performed as a loading control (Invitrogen/Zymed 13-6800).

Cell proliferation assay. The Promega CellTiter 96 AQueous One Solution Cell Proliferation Assay was used, as per the manufacturer's instructions (Promega). Cells were seeded into 96-well plates (1,000 cells per well) in triplicate. Absorbance at 490 nm was measured 2 h after the addition of 20 μL of MTS reagent per well, every 24 h over a 96-h period.

Colony formation in soft agar. A base layer of 1.5% agar/2× DMEM/FBS was prepared in 35-mm plates. Upper layer agar was made using 1.5% agar, 2× DMEM, FBS, and sterile water, and kept in liquid phase in a 42°C water bath. Cells were resuspended in 0.75% agar/DMEM/FBS and overlaid on the base layer with 3,000 cells per 35-mm plate and subsequently kept in a humidified chamber at 37°C for 2 wk. Plates were stained with crystal violet, digitally imaged (Zeiss Axiovert 200 M inverted light microscope), and colony counts performed in an automated fashion using Volocity software particle recognition analysis. Each cell line was plated in triplicate, and the data presented are representative of three separate experiments.

Artificial wound-healing assay. An artificial wound-healing assay was performed to assess cell migratory ability. Cell lines were grown to confluence in medium containing 10% FBS. A uniform scratch defect ("wound") was created across the monolayer using a p10 pipette tip. Wells were then washed with 1× PBS, followed by the addition of serum-free medium. Plates were imaged immediately (t = 0) and at 24 h (t = 24), and the degree to which cells at the wound margin had migrated in to close the initial defect was assessed.

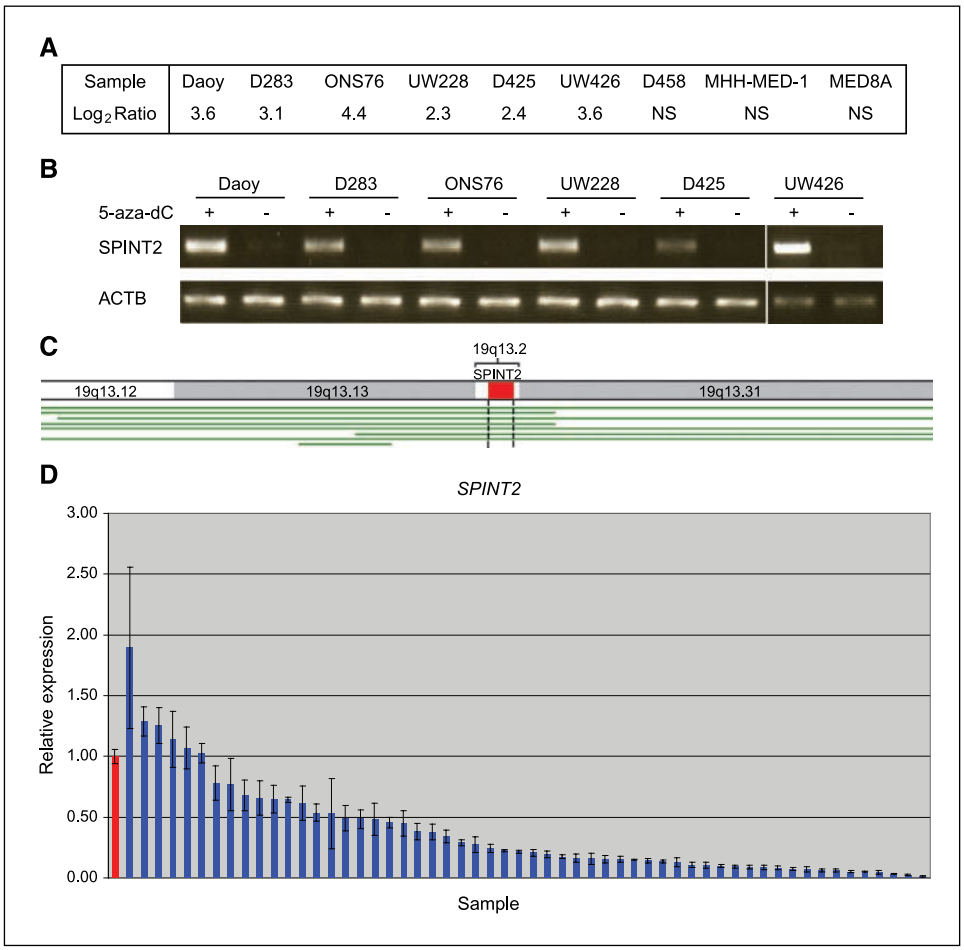

Figure 1. *A,* 5-aza-dC expression microarray data for *SPINT2*, showing $\log_2$ ratios for fold change in expression derived from a pair-wise comparison of 5-aza-dC–treated versus vehicle-treated samples. *NS,* no significant change. *B,* RT-PCR for *SPINT2* in six MB cell lines treated with (+) and without (−) 5-aza-dC showing robust reexpression after treatment. *C,* schematic figure depicting hemizygous deletions encompassing the *SPINT2* locus identified by SNP array. The *SPINT2* locus is indicated by the red box along the chromosome, with samples exhibiting hemizygous deletions depicted by green lines below. One MB cell line (*MED8A*) and six primary MB samples (*MB 7, 9, 22, 23, 29*, and *76*) showed hemizygous loss of *SPINT2* (*region between black dashed lines below chromosome*). *D,* qRT-PCR data for *SPINT2* in pooled normal fetal cerebellum (*red*) and primary MB samples (*blue*). Forty-one of 56 tumors showed *SPINT2* expression levels of <50% compared with normal fetal cerebellum.

Crystal violet focus formation assay. Equal numbers (n = 10,000) of ONS76-Empty Vector and ONS76-*SPINT2*-FLAG cells were plated separately in 10-cm tissue culture plates and grown for a period of 5 d. Plates were then washed twice with ice-cold 1× PBS, fixed for 10 min with ice-cold methanol, and stained with 0.5% crystal violet (made in 25% methanol) for 10 min at room temperature. Plates were then rinsed in ddH_20, allowed to dry, and imaged.

Orthotopic intracranial xenografts. D283 cells stably transfected with empty vector or the D283-*SPINT2*-FLAG-High expression construct were used for xenograft experiments. Cells were released from the culture plates using Accutase (Sigma-Aldrich), washed twice in 1× PBS, resuspended in a small volume of serum-free 1× DMEM, at a final concentration of 50,000 cells/μL, and kept on ice until the time of injection. Mice were anesthetized using i.p. ketamine/xylazine. Intracranial injection of 100,000 cells (2 μL) was performed in the midline cerebellum of male Nu/Foxn1/Nu mice (ages 5–6 wk; Charles River), using a murine stereotactic head frame and Hamilton syringe. Ten mice were injected with D283 cells stably transfected with empty pcDNA3.1+, and 10 mice injected with the D283-*SPINT2*-FLAG-High stable cell line. Mice were observed for evidence of a symptomatic intracranial mass such as domed skull, incoordination, lethargy, or weight loss >20% of maximal body weight. They were then sacrificed. Whole brain specimens, including the cerebellar xenograft tumor, were fixed in 10% formalin for 72 h followed by 70% ethanol until all samples were obtained for further processing. Samples were paraffin embedded, sections were cut and mounted onto slides, and stained for H&E, human SPINT2 (R and D Systems; MAB 1106), cleaved Caspase-3 (Asp175; Cell Signaling Technology), and Ki-67 labeling index. Slides were imaged using a Zeiss Mirax Slide Scanner.

Results

5-aza-dC microarray and SNP array analysis. The 5-aza-dC expression microarray screen identified increased transcript levels for genes known to be methylated in MB, including *CASP8, CDKN2B, DNAJD1, GSTP1, HIC1, RASSF1, S100A6, S100A10, SGNE1, TIMP3*, and *ZIC2* (28–31). To identify novel gene candidates from this microarray screen, we focused on genes demonstrating >2-fold up-regulation in expression after 5-aza-dC treatment, in 2 or more MB cell lines, with predicted promoter-region CpG islands, and which were also identified as targets for deletion or LOH based on SNP array analysis. In addition, we focused on genes known to be TSGs in other tumor types or involved in signaling pathways implicated in cerebellar development or MB pathogenesis. One gene candidate was an inhibitor of HGF/MET signaling, *SPINT2*. It showed between 5.28- and 21.11-fold ($\log_2$ ratios, 2.4–5.4) increase in transcript levels in 6 of 9 MB cell lines (Daoy, D283, ONS76, UW228, UW426, and D425) after 5-aza-dC treatment (Fig. 1*A*). This increased expression after treatment was confirmed by RT-PCR (Fig. 1*B*). These findings suggested that *SPINT2* was silenced by promoter-region methylation in these MB cell lines. In addition to being a target of aberrant promoter methylation, 1 MB cell line (MED8A) and 6 primary MB tumors (MB 7, 9, 22, 23, 29, and 76) showed overlapping regions of focal hemizygous deletion targeting the *SPINT2* locus on chromosome 19q13.2 (Fig. 1*C*). [4] Additional HGF/MET signaling members also exhibited copy number changes

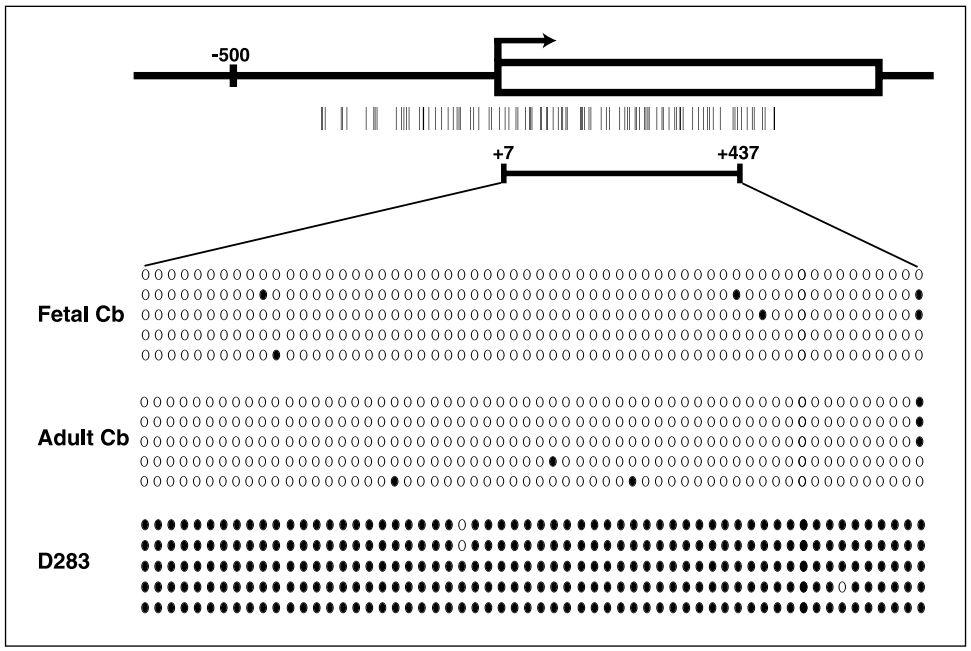

Figure 2. Bisulfite sequencing data for *SPINT2*. The promoter-region, first exon and transcription start site (*arrow*). *Vertical black tick marks,* CG dinucleotides within the promoter-region CpG island. *Horizontal black bar,* the region sequenced, which is expanded below. Each circle represents a single CG dinucleotide site; *open circles,* unmethylated; filled circles, methylated. Each row represents replicate data for the respective sample. The D283 MB cell line shows extensive methylation compared with normal adult and fetal cerebellum (*Cb*).

based on SNP array analysis. Large-scale gains (involving either all of chromosome 7 or the 7q arm) encompassing numerous genes including the *HGF* and *MET* loci (7q21.1 and 7q31, respectively) were seen in 62/201 (30.8%) primary tumors examined on the SNP array platforms.[4]

Quantitative RT-PCR for *SPINT2, MET*, and *HGF*. For a subset of primary tumors, mRNA was available for qRT-PCR analysis of *SPINT2* gene expression. In total, 41 of 56 (73.2%) primary MBs showed >50% reduction in *SPINT2* expression compared with a sample of 5 pooled normal fetal cerebella (Fig. 1*D*). Of 6 primary tumors with hemizygous deletion targeting the *SPINT2* locus, cDNA was available to correlate *SPINT2* expression status in 3 samples (MB 7, 9, and 29). All 3 samples showed reduced *SPINT2* expression compared with normal fetal cerebellum, with 2 of 3 demonstrating expression levels below 50% that of normal cerebellum (MB 7 and 9). Sufficient material was available for 44 primary MBs to assess the expression levels of additional HGF/MET signaling members by qRT-PCR. In this subset of MBs, *MET* receptor expression was up-regulated by 2-fold in 20 of 44 (45.5%) and by over 10-fold in 12 of 44 (27.3%) of samples (Supplementary Fig. S3). Among this group of tumors, 12 had evidence of low copy number gain affecting the *MET* locus by SNP array analysis. Only one tumor with chromosome 7 gain showed increased *MET* gene expression, suggesting that *MET* overexpression may not be copy number driven in human MB. Overexpression of the *HGF* ligand itself was infrequent, with only 1 of 44 (2.3%) of primary tumors examined demonstrating a >2-fold increase in *HGF* expression compared with normal fetal cerebellum (Supplementary Fig. S4).

Bisulfite sequencing and MSP for *SPINT2*. To confirm that the *SPINT2* promoter was densely methylated, bisulfite sequencing was performed. A 901bp promoter-region CpG island surrounds the transcription start site for *SPINT2* (−464 to +437, %GC 70.4, ObsCpG/ExpCpG 0.825). Bisulfite sequencing for a portion of the *SPINT2* CpG island was performed on the D283 MB cell line as well as normal fetal and adult cerebellum, providing information on the methylation status for 57 CG dinucleotides located between +7 and +437 (Fig. 2). In normal cerebellar samples, this CpG island remained largely unmethylated. In contrast, the D283 MB cell line was densely methylated across all CG sites sequenced (Fig. 2).

To identify aberrant *SPINT2* methylation in primary human MB samples, MSP was performed on panel of 70 tumors, in addition to the D283 MB cell line and three normal human cerebellar samples (Fig. 3*A*). As expected, the D283 cell line yielded an MSP product only with primers specific for methylated template. In contrast, three normal cerebellar samples produced MSP product only with primers specific for unmethylated template. Among the primary MB specimens assessed, 24 of 70 (34.3%) yielded MSP product using primers specific for methylated template. qRT-PCR expression data for *SPINT2* was available for 11 of the primary MB specimens that were positive for methylation by MSP. In 10 of 11 (90.9%) tumors, *SPINT2* levels were reduced by over 50%, with 8 of 11 expressing *SPINT2* at levels <10% that of normal fetal cerebellum (Fig. 3*B*).

Effect of *SPINT2* on MB cell proliferation, anchorage-independent growth, and motility. To determine the effect of stable *SPINT2* reexpression on cell proliferation, an MTS assay was performed using D283 and ONS76 cells transfected with empty vector, EGFP, or *SPINT2* expression constructs. As seen in Fig. 4*A*, stable reexpression of *SPINT2* in D283 cells reduced proliferation compared with empty vector and EGFP-expressing controls. In addition, the level of *SPINT2* reexpression correlated inversely with proliferation, with the D283-*SPINT2*-FLAG-Low clone proliferating somewhat more rapidly than the D283-*SPINT2*-FLAG-High clone. Similarly, stable reexpression of SPINT2 in the ONS76 cell line reduced proliferation compared with empty vector or EGFP-expressing controls as assessed by an MTS assay and a Crystal Violet Focus Formation Assay (Supplementary Fig. S5; Fig. 4*A*).

[4] P. Northcott, Y. Nakahara, J. Peacock, D. Ellison, S. Croul, L. Feuk, Y-S. Ra, P. Kongkham, K. Zilberberg, S. Mack, J. Mcleod, S.W. Scherer, J.S. Rao, W. Grajkowska, Y. Gillespie, B. Lach, R. Grundy, I.F. Pollack, R. Hamilton, T. Van Meter, C.G. Carlotti, F. Boop, D. Bigner, R. Gilbertson, J.T. Rutka, and M.D. Taylor. Multiple Recurrent Genetic Events Converge On Control of Histone Lysine Methylation in Medulloblastoma. Submitted for publication.

To assess the effect of stable *SPINT2* reexpression on the ability of the MB cells to grow in anchorage-independent conditions, we tested colony formation in soft agar using the stably transfected D283 cell lines. Empty vector controls produced a mean number of 669.3 ± 50.1 colonies. In contrast, the D283-*SPINT2*-FLAG-High and D283-*SPINT2*-FLAG-Low clones produced mean colony counts of 89.7 ± 18.5 and 274.0 ± 30.8, respectively. There were fewer colonies produced by the high-expressing *SPINT2* clone compared with the low-expressing *SPINT2* clone (Fig. 4*B–C*).

An artificial wound-healing assay was performed to assess the effect of *SPINT2* reexpression on MB cell motility (Fig. 5). Twenty-four hours after the creation of an initial defect in the cell monolayer, the empty vector control displayed over 50% closure of the defect (Fig. 5*A–B*). In contrast, the D283-*SPINT2*-FLAG-High expressing clone showed minimal closure of the initial defect (Fig. 5*C–D*).

Orthotopic intracranial xenografting of stably transfected D283 cell lines. Mice harboring intracerebellar xenografts derived from D283 MB cells stably transfected with empty vector exhibited a mean overall survival (OS) after initial tumor engrafting of 29.3 d (Fig. 6*A*). Mice with xenografts derived from the D283-*SPINT2*-FLAG-High clone showed a mean OS of 64.0 d. The difference in mean OS was statistically significant ($P < 0.0001$). Microscopically, empty vector control xenografts resembled the human anaplastic MB subtype (Fig. 6*B*). Interestingly, *SPINT2* reexpression resulted in regions of intratumoral necrosis not seen in empty vector control–derived tumors (Fig. 6*B*). In addition, *SPINT2*-reexpressing tumors exhibited increased apoptotic activity compared with controls, as shown by increased immunopositivity for cleaved Caspase-3 (Fig. 6*B*). Finally, Ki-67 labeling was reduced from 29.3% ± 3.01% in control tumors to 20.51% ± 1.58% ($P = 0.0012$) in the *SPINT2* transfectant tumors (Fig. 6*B*).

Discussion

To uncover novel TSGs involved in MB pathogenesis, we used a genome-wide approach using 5-aza-dC treatment to interrogate the MB epigenome in 9 MB cell lines. We identified for the first time the inhibitor of HGF/MET signaling, *SPINT2*, as a novel candidate TSG in MB. The first genome-wide approach to the MB

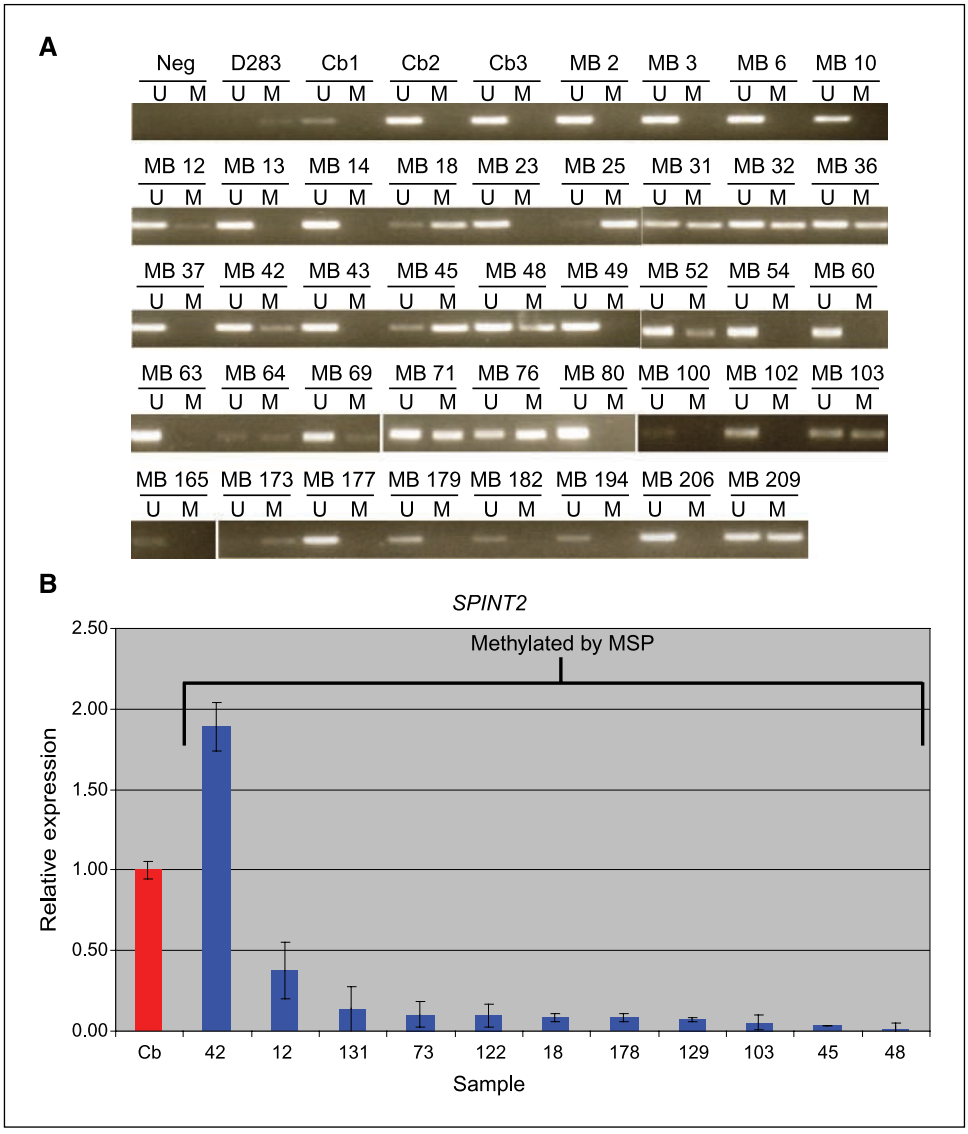

Figure 3. *A,* representative MSP data for *SPINT2*. *U,* unmethylated-specific primers. *M,* methylated-specific primers. *Neg,* no template control. *D283,* D283 MB cell line. *Cb,* normal cerebellum. *MB,* primary MB samples. The D283 MB cell line produces a band only with methylated-specific primers. Normal cerebellar samples produce MSP product only with primers specific for unmethylated template. In total, 34.3% (24 of 70) primary MB tumor samples were positive for *SPINT2* methylation. *B,* qRT-PCR data for *SPINT2* expression in primary MB samples identified as methylated by MSP. Ten of 11 (90.9%) tumors with *SPINT2* methylation show reduced *SPINT2* expression.

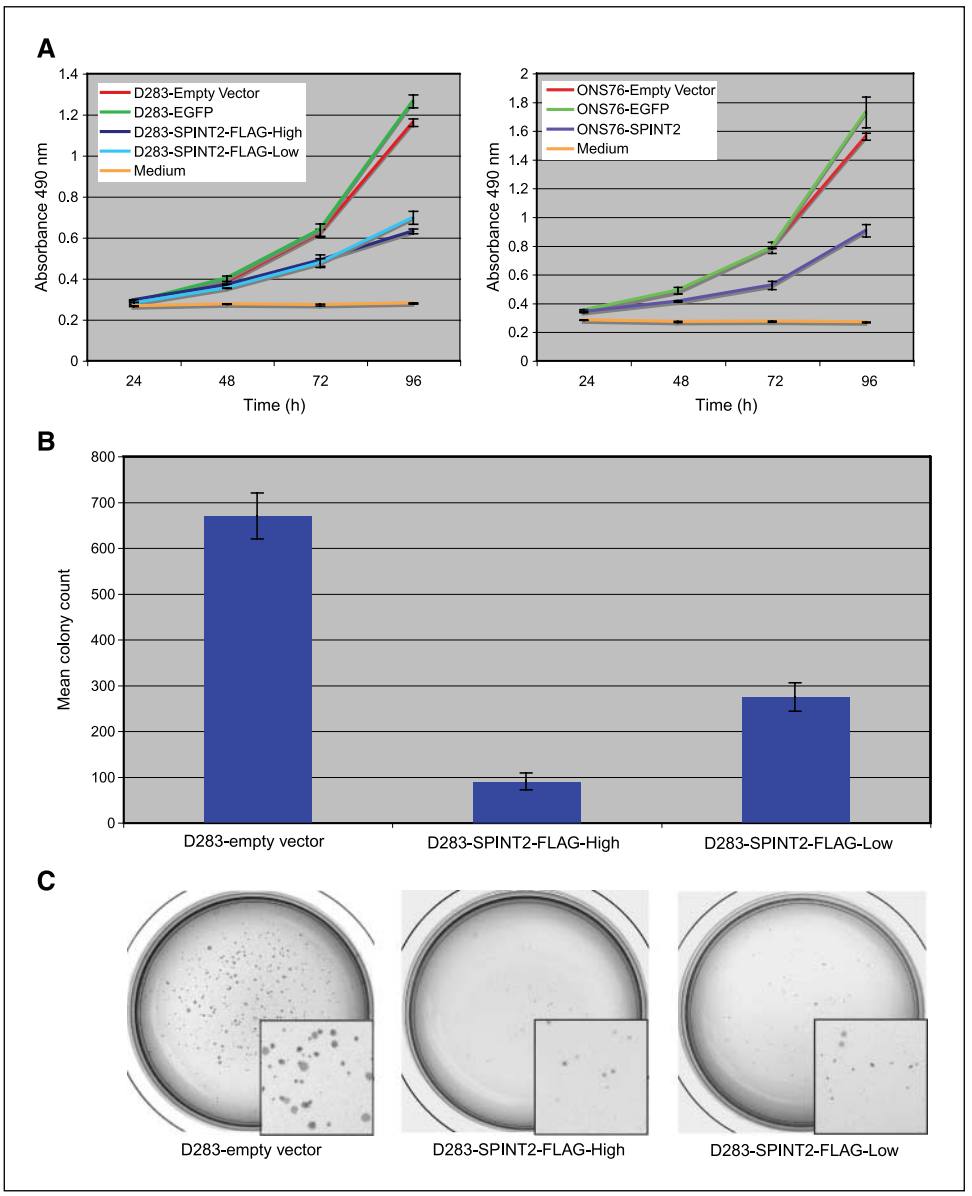

Figure 4. *A,* stable *SPINT2* reexpression (D283-*SPINT2*-FLAG-High, D283-*SPINT2*-FLAG-Low, and ONS76-*SPINT2*-FLAG) significantly reduced D283 and ONS76 MB cell proliferation as assessed by MTS assay compared with empty vector–transfected or EGFP-expressing controls. *B,* stable *SPINT2* reexpression reduced colony formation in soft agar compared with empty vector controls. *C,* representative 35-mm plates from soft agar assay for empty vector controls, D283-*SPINT2*-FLAG-High, and D283-*SPINT2*-FLAG-Low cells. *Inserts,* a portion of each plate that has been enlarged (×5).

epigenome performed by Fruhwald and colleagues (32) identified aberrant methylation affecting ~6% and 1% of genes in MB cell lines and primary tumors respectively. Three additional genome-wide studies have been published (29, 30, 33). Waha and colleagues (30) performed a differential methylation hybridization technique, from which they identified secretory granule neuroendocrine protein 1 (*SGNE1/7B2*) as a putative TSG that is methylated in MB. Using a technique called array-based profiling of reference-independent methylation status, Pfister (29) identified zinc-finger protein of the cerebellum family member 2 (*ZIC2*) as being methylated in a subset of 20 MB specimens. A genome-wide approach examining 3 MB cell lines recently published by Anderton (33) identified tumor-specific methylation of the *COL1A2, S100A10, S100A6, HTATIP2, CDH1*, and *LXN* genes. Furthermore, they identified a clinicopathologic correlation for *COL1A2* methylation, which, although common in nondesmoplastic/nodular MBs of all ages and desmoplastic/nodular MBs of childhood, is a rare occurrence among desmoplastic/nodular MBs of infancy (33). Our epigenome-wide study examining 9 MB cell lines and 201 primary tumors adds to the list of epigenetically silenced genes, identifying *SPINT2* as a putative TSG targeted frequently for promoter-region methylation-mediated silencing, and further implicates the HGF/MET signaling pathway in this disease.

HGF/MET signaling plays a role in cerebellar development, contributing to cerebellar granule cell precursor (GCP) proliferation and survival (17, 34–36). HGF and MET are expressed in the developing and adult cerebellum (34, 35). Murine cerebellar GCPs proliferate *in vitro* in response to exogenous Hgf (17). *In vitro* stimulation of Hgf/Met signaling also prevents apoptosis of GCPs induced by serum starvation (36). In contrast, the *reduced* Hgf/Met signaling seen in a murine hypomorphic *Met*

mutant produces a small cerebellum with foliation defects in the central and posterior cerebellar vermis (17). Furthermore, the reduced Hgf/Met signaling in this model results in GCP proliferation that is 25% lower than wild-type GCPs (17).

Aberrant HGF/MET signaling has been implicated in brain tumor pathogenesis through its influence on cell cycle progression, tumor cell migration and invasion, angiogenesis, and protection from apoptotic stimuli (16). This pathway, however, has only recently been implicated in MB pathogenesis (15, 18, 19). Using CGH and array-CGH methods, Tong and colleagues (15) identified single copy gains encompassing the *MET* locus on chromosome 7q in 38.5% of samples in a cohort of 13 human MBs. By lower resolution CGH alone, they identified gain of the entire 7q chromosome arm in 4 samples and gain of the 7q31-35 region in 1 tumor (15). We similarly identified large-scale gains affecting either all of chromosome 7 or the 7q arm based on SNP array analysis in 62 of 201 (30.8%) primary MBs. We did not however observe any high-level amplifications targeting the *MET* or *HGF* loci. Interestingly, in our study, increased *HGF* or *MET* gene expression did not correlate with copy number gain, suggesting that *HGF* and *MET* expression are not copy number driven, and that these genes are not driving clonal selection in tumors with gains on chromosome 7.

Li and colleagues (19) identified MET receptor and HGF expression in MB cell lines and primary tumors. They showed that up-regulation of HGF/MET signaling increased cell proliferation, anchorage-independent growth, cell-cycle progression, and resistance to chemotherapy-induced apoptosis in MB cell lines (19). In addition, after HGF treatment, the Daoy MB cell line exhibited a more aggressive, anaplastic phenotype (19). Furthermore, high MET expression in primary tumors correlated with reduced OS (19). More recently, Li and colleagues (18) identified a link between HGF/MET signaling and *MYCC* in MB. Despite these initial studies, the extent to which aberrant HGF/MET signaling contributes to MB, as well as the diverse mechanisms by which this pathway may be dysregulated, remain to be determined.

Based on the results of our screen, *SPINT2* was chosen for further study for multiple reasons. *SPINT2* was up-regulated after 5-aza-dC in 6 of 9 MB cell lines and was a recurrent target of hemizygous deletion based on SNP array analysis. In addition, by qRT-PCR analysis, *SPINT2* expression was reduced by >50% in 41 of 56 (73.2%) primary MBs compared with normal fetal cerebellum. Furthermore, *SPINT2* functions as a TSG activity and is silenced by promoter-region methylation in hepatocellular carcinoma, renal cell carcinoma, and gliomas (27, 37, 38). In addition, low *SPINT2* expression has been associated with more advanced stage malignancy and poor prognosis in breast cancer (39). The HGF/MET pathway has an established role in normal cerebellar development (17). Finally, although the HGF/MET oncogenic signaling pathway has recently been implicated in MB pathogenesis (18, 19), the role of *SPINT2* in MB has not yet been examined.

The SPINT2 protein is one of two known inhibitors of HGF activator (HGFA; refs. 40, 41). HGFA is a protease that converts the inactive, single-chain precursor form of HGF to its active heterodimeric form, which can then bind to the MET receptor (16, 42). By inhibiting the activation of HGF by HGFA, SPINT2 limits signaling via the HGF/MET pathway. Epigenetic silencing of *SPINT2* may allow HGF/MET signaling to continue without inhibition, contributing to the malignant phenotype.

Similar to *SPINT2*, an additional HGFA inhibitor (*SPINT1*) also showed >2-fold increase in expression by 5-aza-dC microarray analysis (3 of 9 cell lines; Supplementary Fig. S6). Bisulfite sequencing confirmed promoter methylation in the UW228 MB cell line (Supplementary Fig. S6). Despite this, MSP on primary MBs failed to identify *SPINT1* promoter methylation, raising the question of whether *SPINT1* methylation in MB cell lines was biologically significant or an artifact of cell culture (data not shown). Furthermore, qRT-PCR analysis of *SPINT1* and *SPINT2* expression

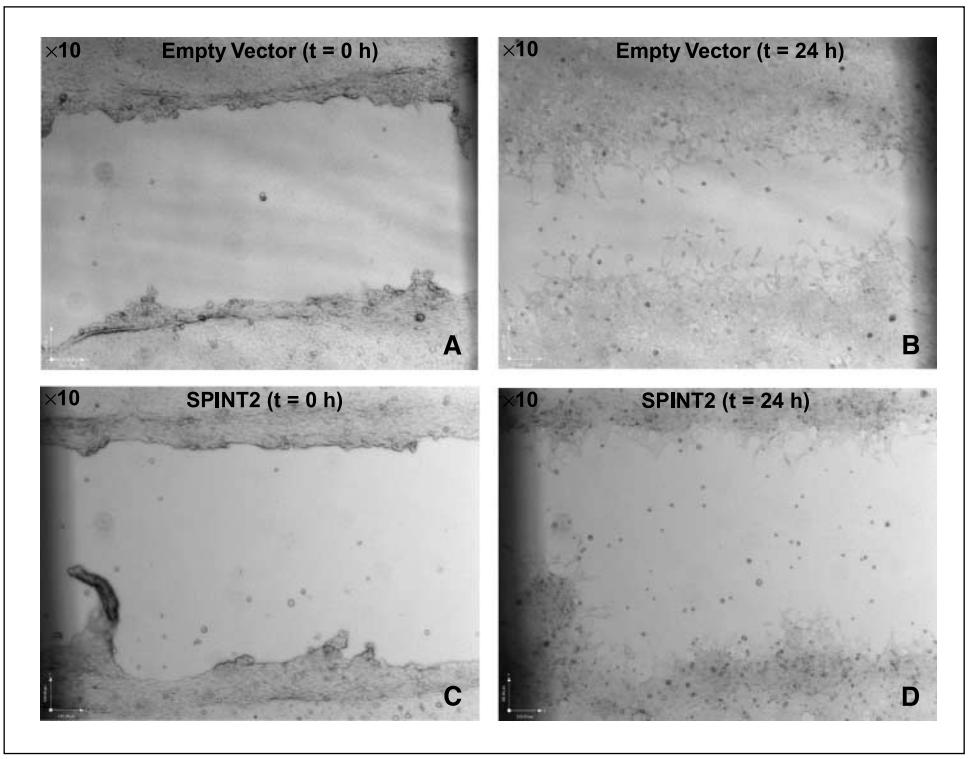

Figure 5. Artificial wound-healing assay. Initial defect in cell monolayer (time = 0) for D283 MB cells stably transfected with empty vector (*A*) and D283-*SPINT2*-FLAG-High (*C*). Twenty-four hours after the creation of the initial defect, empty vector–transfected control cells show over 50% closure of the defect (*B*), compared with minimal closure for the *SPINT2*-reexpressing clone (*D*).

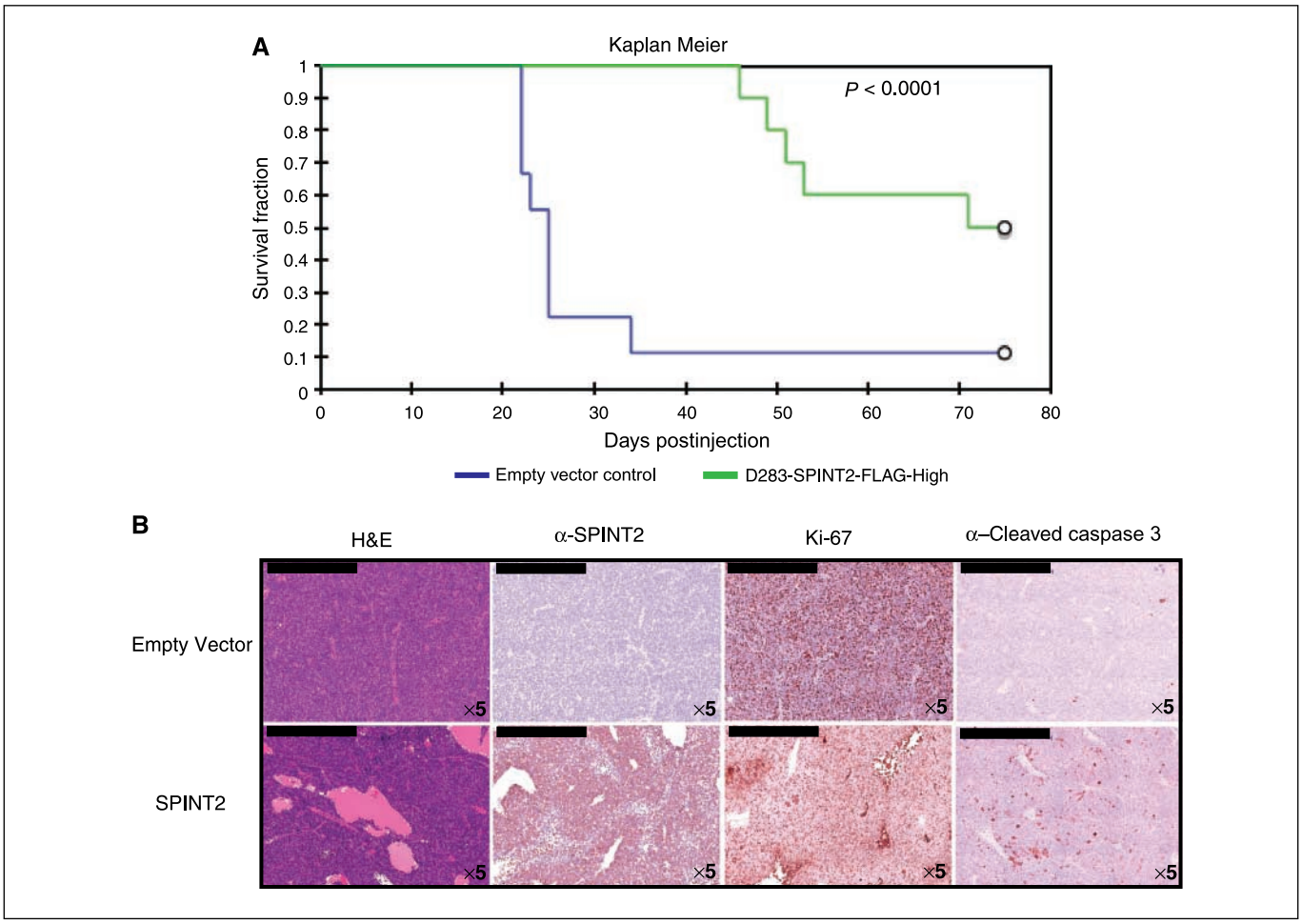

Figure 6. *A,* Kaplan Meier survival curve for orthotopic intracerebellar xenografts. Reexpression of *SPINT2* approximately doubled OS after intracranial xenografting ($P < 0.0001$). *B,* immunohistochemistry for xenograft tumor samples. *SPINT2*-reexpressing D283 cells showed central regions of cystic necrosis, increased immunopositivity for cleaved Caspase-3 (Asp175), and a reduced Ki-67 labeling index in comparison with empty vector–transfected D283 cells (*Bar,* 500 μm).

in normal fetal cerebellum showed *SPINT2* expression to be ~4.5-fold higher than *SPINT1* (Supplementary Fig. S7). Therefore, one might infer that *SPINT2* serves as the primary biologically relevant inhibitor of HGF/MET signaling in the cerebellum.

After identifying increased *SPINT2* expression with 5-aza-dC treatment in 6 of 9 MB cell lines, *SPINT2* promoter methylation was confirmed by bisulfite sequencing in the D283 MB cell line, in comparison with normal human fetal and adult cerebellar samples that are unmethylated. MSP showed *SPINT2* methylation in 34.3% (24 of 70) of primary MBs.

In vitro analysis supported a role of *SPINT2* as a TSG in MB, as stable reexpression in the D283 MB cell line reduced proliferative capacity, anchorage-independent growth, and cell motility *in vitro*. Stable reexpression of *SPINT2* in the ONS76 MB cell line similarly reduced its proliferative capacity *in vitro*. Furthermore, mice harboring intracerebellar xenografts derived from *SPINT2*-reexpressing D283 cells showed survival times more than double that of mice engrafted with empty vector–transfected cells. Immunohistochemical analysis of xenograft samples provided some explanation for the prolonged survival of mice harboring *SPINT2*-reexpressing xenografts. Intratumoral necrosis was widespread in xenograft specimens from *SPINT2* transfectants. Furthermore, *SPINT2*-reexpressing xenografts showed increased apoptotic activity as evidenced by increased immunopositivity for cleaved Caspase-3 compared with controls. Given that HGF treatment confers resistance to chemotherapy-induced apoptosis in Daoy cells and resistance to apoptosis in serum-starved GCPs, one explanation for this finding may be sensitization to apoptotic stimuli in the *SPINT2* transfectants (19, 36). Finally, *SPINT2* xenografts showed reduced Ki-67 staining compared with empty-vector controls—a marker of reduced proliferation *in vivo*.

We identify *SPINT2* as a putative TSG involved in MB pathogenesis, and show promoter-region methylation-mediated epigenetic silencing of this gene in MB. In addition, this work contributes to the body of evidence implicating the HGF/MET oncogenic signaling pathway in MB pathogenesis. We have uncovered another mechanism for uncontrolled HGF/MET signaling in this tumor. In fact, reduced *SPINT2* expression seems to be a more frequent event in primary MB than either *HGF* or *MET* overexpression. Our study shows that dysregulation of HGF/MET signaling due to loss of normal pathway inhibition is a frequent event in MB, providing some rationale for targeting this signaling axis in MB with current and future therapeutic interventions (43–47).

Disclosure of Potential Conflicts of Interest

No potential conflicts of interest were disclosed.

Acknowledgments

Received 6/9/2008; revised 9/5/2008; accepted 9/24/2008.

Grant support: Canadian Cancer Society, National Cancer Institute of Canada (019073), the Pediatric Brain Tumor Foundation, the Wiley Fund at the Hospital for Sick Children, and B.r.a.i.n.child. J.T. Rutka is a scientist of the Canadian Institutes of Health Research. P.N. Kongkham was supported by the Surgeon Scientist Program in the Department of Surgery, the University of Toronto, a National Cancer Institute of Canada Terry Fox Foundation clinical research fellowship and a research studentship from RESTRACOMP, The Hospital for Sick Children, Toronto.

The costs of publication of this article were defrayed in part by the payment of page charges. This article must therefore be hereby marked *advertisement* in accordance with 18 U.S.C. Section 1734 solely to indicate this fact.

References

1. Schoenberg BS, Schoenberg DG, Christine BW, Gomez MR. The epidemiology of primary intracranial neoplasms of childhood. A population study. Mayo Clin Proc 1976;51:51–6.
2. Park TS, Hoffman HJ, Hendrick EB, Humphreys RP, Becker LE. Medulloblastoma: clinical presentation and management. Experience at the hospital for sick children, toronto, 1950-1980. J Neurosurg 1983;58:543–52.
3. Roberts RO, Lynch CF, Jones MP, Hart MN. Medulloblastoma: a population-based study of 532 cases. J Neuropathol Exp Neurol 1991;50:134–44.
4. Glauser TA, Packer RJ. Cognitive deficits in long-term survivors of childhood brain tumors. Childs Nerv Syst 1991;7:2–12.
5. Duffner PK, Cohen ME, Thomas P. Late effects of treatment on the intelligence of children with posterior fossa tumors. Cancer 1983;51:233–7.
6. Mulhern RK, Kepner JL, Thomas PR, Armstrong FD, Friedman HS, Kun LE. Neuropsychologic functioning of survivors of childhood medulloblastoma randomized to receive conventional or reduced-dose craniospinal irradiation: a Pediatric Oncology Group study. J Clin Oncol 1998;16:1723–8.
7. Clayton PE, Shalet SM. Dose dependency of time of onset of radiation-induced growth hormone deficiency. J Pediatr 1991;118:226–8.
8. Johnson RL, Rothman AL, Xie J, et al. Human homolog of patched, a candidate gene for the basal cell nevus syndrome. Science 1996;272:1668–71.
9. Hamilton SR, Liu B, Parsons RE, et al. The molecular basis of Turcot's syndrome. N Engl J Med 1995;332:839–47.
10. Raffel C, Jenkins RB, Frederick L, et al. Sporadic medulloblastomas contain PTCH mutations. Cancer Res 1997;57:842–5.
11. Taylor MD, Liu L, Raffel C, et al. Mutations in SUFU predispose to medulloblastoma. Nat Genet 2002;31:306–10.
12. Reifenberger J, Wolter M, Weber RG, et al. Missense mutations in SMOH in sporadic basal cell carcinomas of the skin and primitive neuroectodermal tumors of the central nervous system. Cancer Res 1998;58:1798–803.
13. Smyth I, Narang MA, Evans T, et al. Isolation and characterization of human patched 2 (PTCH2), a putative tumour suppressor gene inbasal cell carcinoma and medulloblastoma on chromosome 1p32. Hum Mol Genet 1999;8:291–7.
14. Mori T, Nagase H, Horii A, et al. Germ-line and somatic mutations of the APC gene in patients with Turcot syndrome and analysis of APC mutations in brain tumors. Genes Chromosomes Cancer 1994;9:168–72.
15. Tong CY, Hui AB, Yin XL, et al. Detection of oncogene amplifications in medulloblastomas by comparative genomic hybridization and array-based comparative genomic hybridization. J Neurosurg 2004;100:187–93.
16. Abounader R, Laterra J. Scatter factor/hepatocyte growth factor in brain tumor growth and angiogenesis. Neuro-oncol 2005;7:436–51.
17. Ieraci A, Forni PE, Ponzetto C. Viable hypomorphic signaling mutant of the Met receptor reveals a role for hepatocyte growth factor in postnatal cerebellar development. Proc Natl Acad Sci U S A 2002;99:15200–5.
18. Li Y, Guessous F, Johnson EB, et al. Functional and molecular interactions between the HGF/c-Met pathway and c-Myc in large-cell medulloblastoma. Lab Invest 2008;88:98–111.
19. Li Y, Lal B, Kwon S, et al. The scatter factor/hepatocyte growth factor: c-met pathway in human embryonal central nervous system tumor malignancy. Cancer Res 2005;65:9355–62.
20. Karpf AR, Peterson PW, Rawlins JT, et al. Inhibition of DNA methyltransferase stimulates the expression of signal transducer and activator of transcription 1, 2, and 3 genes in colon tumor cells. Proc Natl Acad Sci U S A 1999;96:14007–12.
21. Yamashita K, Upadhyay S, Osada M, et al. Pharmacologic unmasking of epigenetically silenced tumor suppressor genes in esophageal squamous cell carcinoma. Cancer Cell 2002;2:485–95.
22. Suzuki H, Gabrielson E, Chen W, et al. A genomic screen for genes upregulated by demethylation and histone deacetylase inhibition in human colorectal cancer. Nat Genet 2002;31:141–9.
23. Zardo G, Tiirikainen MI, Hong C, et al. Integrated genomic and epigenomic analyses pinpoint biallelic gene inactivation in tumors. Nat Genet 2002;32:453–8.
24. Clark SJ, Harrison J, Paul CL, Frommer M. High sensitivity mapping of methylated cytosines. Nucleic Acids Res 1994;22:2990–7.
25. Bock C, Reither S, Mikeska T, Paulsen M, Walter J, Lengauer T. BiQ Analyzer: visualization and quality control for DNA methylation data from bisulfite sequencing. Bioinformatics 2005;21:4067–8.
26. Herman JG, Graff JR, Myohanen S, Nelkin BD, Baylin SB. Methylation-specific PCR: a novel PCR assay for methylation status of CpG islands. Proc Natl Acad Sci U S A 1996;93:9821–6.
27. Morris MR, Gentle D, Abdulrahman M, et al. Tumor suppressor activity and epigenetic inactivation of hepatocyte growth factor activator inhibitor type 2/SPINT2 in papillary and clear cell renal cell carcinoma. Cancer Res 2005;65:4598–606.
28. Lindsey JC, Anderton JA, Lusher ME, Clifford SC. Epigenetic events in medulloblastoma development. Neurosurg Focus 2005;19:E10.
29. Pfister S, Schlaeger C, Mendrzyk F, et al. Array-based profiling of reference-independent methylation status (aPRIMES) identifies frequent promoter methylation and consecutive downregulation of ZIC2 in pediatric medulloblastoma. Nucleic Acids Res 2007;35:e51.
30. Waha A, Koch A, Hartmann W, et al. SGNE1/7B2 is epigenetically altered and transcriptionally downregulated in human medulloblastomas. Oncogene 2007;26:5662–8.
31. Lindsey JC, Lusher ME, Strathdee G, et al. Epigenetic inactivation of MCJ (DNAJD1) in malignant paediatric brain tumours. Int J Cancer 2006;118:346–52.
32. Fruhwald MC, O'Dorisio MS, Dai Z, et al. Aberrant promoter methylation of previously unidentified target genes is a common abnormality in medulloblastomas-implications for tumor biology and potential clinical utility. Oncogene 2001;20:5033–42.
33. Anderton JA, Lindsey JC, Lusher ME, et al. Global analysis of the medulloblastoma epigenome identifies disease subgroup-specific inactivation of COL1A2. Neuro-oncol 2008. Epub 2008 Jul 29.
34. Honda S, Kagoshima M, Wanaka A, Tohyama M, Matsumoto K, Nakamura T. Localization and functional coupling of HGF and c-Met/HGF receptor in rat brain: implication as neurotrophic factor. Brain Res Mol Brain Res 1995;32:197–210.
35. Jung W, Castren E, Odenthal M, et al. Expression and functional interaction of hepatocyte growth factor-scatter factor and its receptor c-met in mammalian brain. J Cell Biol 1994;126:485–94.
36. Zhang L, Himi T, Morita I, Murota S. Hepatocyte growth factor protects cultured rat cerebellar granule neurons from apoptosis via the phosphatidylinositol-3 kinase/Akt pathway. J Neurosci Res 2000;59:489–96.
37. Fukai K, Yokosuka O, Chiba T, et al. Hepatocyte growth factor activator inhibitor 2/placental bikunin (HAI-2/PB) gene is frequently hypermethylated in human hepatocellular carcinoma. Cancer Res 2003;63:8674–9.
38. Schuster JM, Longo M, Nelson PS. Differential expression of bikunin (HAI-2/PB), a proposed mediator of glioma invasion, by demethylation treatment. J Neurooncol 2003;64:219–25.
39. Parr C, Watkins G, Mansel RE, Jiang WG. The hepatocyte growth factor regulatory factors in human breast cancer. Clin Cancer Res 2004;10:202–11.
40. Shimomura T, Denda K, Kitamura A, et al. Hepatocyte growth factor activator inhibitor, a novel Kunitz-type serine protease inhibitor. J Biol Chem 1997;272:6370–6.
41. Kawaguchi T, Qin L, Shimomura T, et al. Purification and cloning of hepatocyte growth factor activator inhibitor type 2, a Kunitz-type serine protease inhibitor. J Biol Chem 1997;272:27558–64.
42. Miyazawa K, Shimomura T, Kitamura A, Kondo J, Morimoto Y, Kitamura N. Molecular cloning and sequence analysis of the cDNA for a human serine protease reponsible for activation of hepatocyte growth factor. Structural similarity of the protease precursor to blood coagulation factor XII. J Biol Chem 1993;268:10024–8.
43. Michieli P, Mazzone M, Basilico C, et al. Targeting the tumor and its microenvironment by a dual-function decoy Met receptor. Cancer Cell 2004;6:61–73.
44. Christensen JG, Schreck R, Burrows J, et al. A selective small molecule inhibitor of c-Met kinase inhibits c-Met-dependent phenotypes *in vitro* and exhibits cytoreductive antitumor activity *in vivo*. Cancer Res 2003;63:7345–55.
45. Cao B, Su Y, Oskarsson M, et al. Neutralizing monoclonal antibodies to hepatocyte growth factor/scatter factor (HGF/SF) display antitumor activity in animal models. Proc Natl Acad Sci U S A 2001;98:7443–8.
46. Brockmann MA, Papadimitriou A, Brandt M, Fillbrandt R, Westphal M, Lamszus K. Inhibition of intracerebral glioblastoma growth by local treatment with the scatter factor/hepatocyte growth factor-antagonist NK4. Clin Cancer Res 2003;9:4578–85.
47. Abounader R, Lal B, Luddy C, et al. *In vivo* targeting of SF/HGF and c-met expression via U1snRNA/ribozymes inhibits glioma growth and angiogenesis and promotes apoptosis. FASEB J 2002;16:108–10.

An Epigenetic Genome-Wide Screen Identifies *SPINT2* as a Novel Tumor Suppressor Gene in Pediatric Medulloblastoma

Paul N. Kongkham, Paul A. Northcott, Young Shin Ra, et al.

Cancer Res 2008;68:9945-9953.